Optical-bias effect on transient electron-drift measurements in *a*-Si:H: Implications on the distribution and capture cross sections of the dangling bonds

C. Longeaud and J. P. Kleider
Laboratoire de Génie Electrique de Paris, Ecole Supérieure d'Electricité, Universités Paris VI et XI, Plateau de Moulon, 91192 Gif-sur-Yvette Cedex, France
(Received 14 March 1996)

The previously reported enhancement of the transient electron-drift signal in hydrogenated amorphous silicon under increasing optical bias, along with the puzzling independence from optical bias of the density of neutral dangling bonds at room temperature, are explained without the need of introducing *ad hoc* slow-relaxation phenomena. Implications on the energy distribution of the dangling bonds and on their capture cross sections are given. [S0163-1829(96)51320-2]

Though a lot of work has been done in the field of hydrogenated amorphous silicon (*a*-Si:H), there are still controversies regarding the defect distribution in this material and the consequences on the electronic properties. For instance, from thermodynamical calculations, several authors proposed a defect-pool model to account for the formation of dangling bonds (DB's) and to explain the evolution of the defect density upon doping, thermal quenching, or light soaking.[1,2] For undoped *a*-Si:H, the model predicts that there are essentially fewer neutral defects than charged ones. However, from modulated photocurrent experiments, it has been recently found that the number of neutral defects exceeds that of charged defects by a factor of the order of ten.[3] Another point of controversy concerns the values of the capture cross sections of the defects. For instance, the ratio σ_n^+/σ_n^0 of the capture cross section of positively charged DB centers (D^+) to that of neutral DB centers (D^0) has been found to be either of the order of 100 (Refs. 3 and 4) or smaller than 5.[5,6]

Recently, it was claimed that the kinetics of relaxation of the defect energy levels after trapping of an electron is extremely slow,[7] and that this slow kinetics could explain some puzzling results obtained from techniques studying transport mechanisms in *a*-Si:H. In particular, in transient electron-drift measurements, it was found by several research groups that the electron-drift signal following deep trapping increases under increasing optical bias.[8,9] Han, Melcher, Schiff, and Silver analyzed this phenomenon in a recent paper,[10] and proposed that defect relaxation under optical bias leads to a shift of the defect energy level towards the conduction band, resulting in a decrease of the deep trapping efficiency. They argued that the simple alternative explanation based on a splitting of the quasi Fermi levels would be incompatible with two experimental observations: (i) the optical-bias-dependent effect occurs even at low intensities (for generation rates as low as 10^{17} cm^{-3} s^{-1}) and (ii) the electron spin resonance (ESR) signal measured on intrinsic *a*-Si:H samples, which is sensitive to the concentration $[D^0]$ of neutral DB centers, is found to be nearly independent of the optical bias at room temperature.[11]

In this paper, we show that the above optical-bias-related phenomena can be well accounted for using the plausible assumption of a broad DB state distribution, kept independent of the optical bias, and a high ratio of electron capture cross sections of positive to neutral defects, provided that the occupation of the amphoteric DB states under illumination is properly taken into account. Consequently, the optical bias data do not require the introduction of physical phenomena such as defect relaxation.

Our analysis is based on a numerical simulation including all electronic transitions from the dangling bonds and band tails with the extended conduction- and valence-band states. In this simulation one can choose the density of states (DOS), the capture cross sections of the states, and the ''experimental'' parameters such as the photon flux of the optical bias, $F_{\rm dc}$, and the temperature T. The main steps of the simulation are the following:

(i) The energy variations of the occupation functions of both the DB states and the monovalent band tail states are derived at given values of $F_{\rm dc}$ and T according to our recent calculation.[12] We can thus calculate the value of $[D^0]$ under optical bias and compare it to that obtained in the dark.

(ii) Electron-hole pairs are injected into the material at $t=0$ in very low densities ($\delta n_0=\delta p_0=10^{+5}$ cm^{-3}). The time dependence of the densities of extra electrons and holes, $\delta n(t)$ and $\delta p(t)$, respectively, is calculated taking all trapping and recombination events into account. We then deduce the variations with the time t of $\mu_n\tau_n(t)=\int_0^t \mu_n[\delta n(t')/\delta n_0]dt'$, μ_n being the electron mobility in the extended states. These variations are equal to that of $Q(t)d^2/Q_0V$ recorded by Han *et al.* in the electron-drift experiment,[10] provided the quantum efficiency η is equal to 1 and the electrons give the dominant contribution to the transient current. This latter point is verified in our simulation because the valence-band tail is larger than the conduction-band tail, and the hole mobility was chosen to be smaller than that of the electrons ($\mu_p=1$ cm^2 V^{-1} s^{-1} and $\mu_n=10$ cm^2 V^{-1} s^{-1}), in agreement with what is usually assessed in *a*-Si:H.

For the simulations presented herein the temperature was chosen to be equal to 300 K and the flux $F_{\rm dc}$ was varied between 10^9 and 3.2×10^{15} cm^{-2} s^{-1}. The Tauc gap E_g was taken to be equal to 1.8 eV. The DOS was made of two exponential band tails of monovalent states and a deep defect

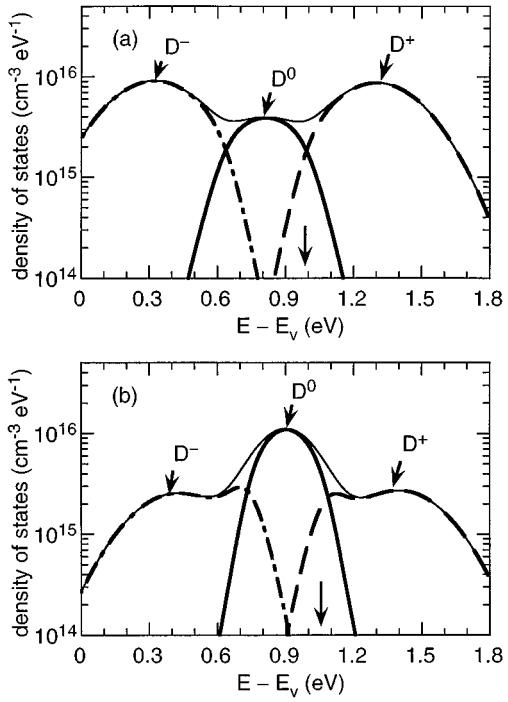

FIG. 1. Distributions of dangling-bond states calculated (a) according to the defect-pool model of Ref. 1, and (b) from the sum of a defect-pool distribution and an extra Gaussian distribution. The position of the dark Fermi level is indicated by an arrow. The bold dashed, solid, and dash-dotted lines correspond to the positively charged, neutral, and negatively charged states, respectively. The thin solid line represents the whole DB density of states. In (a) the ratio of positively charged to neutral dangling bonds is of the order of 3, whereas in (b) it is of the order of 0.5.

distribution of amphoteric dangling bonds. The characteristic temperatures of the conduction- and valence-band tails were chosen to be equal to $T_c = 300$ K and $T_v = 500$ K, respectively. In order to change the relative densities of neutral and charged DB centers, the two types of DB distributions shown in Fig. 1 were tested in our simulation. The first distribution, shown in Fig. 1(a), is calculated from the defect-pool model[1] using the following parameters: frozen-in temperature $T^* = 450$ K, energy position of the pool maximum $E_{\text{pool}} - E_v = 1.3$ eV, standard deviation of the pool $\sigma_{\text{pool}} = 0.2$ eV, correlation energy $U = 0.3$ eV, and hydrogen concentration $[H] = 5 \times 10^{21}$ cm^{-3}. One can see that $[D^0]$ is lower than $[D^+]$ ($[D^0] = 1.37 \times 10^{15}$ cm^{-3} and $[D^+] = 4.12 \times 10^{15}$ cm^{-3}), and corresponds to a low value obtained on device-grade intrinsic *a*-Si:H. The second distribution, shown in Fig. 1(b), is the sum of a distribution calculated from the defect-pool model and a Gaussian distribution centered at midgap ($E_{\max} - E_v = 0.9$ eV). In order to get $[D^0]$ higher than $[D^+]$, we lowered the number of charged states in the defect-pool distribution by increasing the energy of the pool maximum up to $E_{\text{pool}} - E_v = 1.4$ eV, the other pool parameters being the same as in Fig. 1(a). The extra Gaussian distribution has a standard deviation of 0.13 eV and a maximum value $N_{\max} = 10^{16}$ cm^{-3} eV^{-1}. All the DB centers have the same correlation energy and the same capture cross sections. Thus, the sum of the defect-pool and Gaussian distributions behaves as a single species of DB centers. The whole concentrations of neutral and positively charged DB's in the dark are $[D^0] = 2.9 \times 10^{15}$ cm^{-3} and $[D^+] = 1.60 \times 10^{15}$ cm^{-3}, respectively.

TABLE I. Evolution of the concentration of the neutral dangling-bond states $[D^0]$ with the optical bias F_{dc} for the two defect distributions *A* and *B* of Figs. 1(a) and 1(b), respectively. The results are given for two sets of electron capture cross sections of the positively charged and neutral dangling bonds: $\sigma_n^+ = 4 \times 10^{15}$ cm^2 and $\sigma_n^0 = 8 \times 10^{16}$ cm^2 ($R = 5$), and $\sigma_n^+ = 1 \times 10^{14}$ cm^2 and $\sigma_n^0 = 1 \times 10^{16}$ cm^2 ($R = 100$).

F_{dc} (cm^{-2} s^{-1})	$[D^0]_A$ (cm^{-3}) ($R=5$)	$[D^0]_A$ (cm^{-3}) ($R=100$)	$[D^0]_B$ (cm^{-3}) ($R=5$)	$[D^0]_B$ (cm^{-3}) ($R=100$)
0	1.37×10^{15}	1.37×10^{15}	2.91×10^{15}	2.91×10^{15}
1.0×10^{9}	1.75×10^{15}	2.12×10^{15}	2.96×10^{15}	3.13×10^{15}
2.0×10^{10}	2.26×10^{15}	2.83×10^{15}	3.16×10^{15}	3.48×10^{15}
4.0×10^{11}	2.97×10^{15}	3.67×10^{15}	3.36×10^{15}	3.76×10^{15}
8.0×10^{12}	3.66×10^{15}	4.54×10^{15}	3.40×10^{15}	3.94×10^{15}
1.6×10^{14}	4.19×10^{15}	5.13×10^{15}	3.14×10^{15}	3.82×10^{15}
3.2×10^{15}	4.00×10^{15}	5.21×10^{15}	3.20×10^{15}	3.31×10^{15}

We first address the variations of $[D^0]$ with the optical bias for the two distributions of DB states shown in Fig. 1. The variations of $[D^0]$ with the optical bias are reported in Table I. These variations were calculated for two sets of electron capture cross sections, for which the ratio $R = \sigma_n^+ / \sigma_n^0$ of the electron capture cross sections of the positively charged and neutral DB states was equal to 5 and 100, respectively. Obviously, the changes of $[D^0]$ with F_{dc} are very weak for the distribution of Fig. 1(b) (35% at most), whereas a strong increase is observed for that of Fig. 1(a) (a factor of 3 to 4 depending on *R*). This result indicates that when the ratio $[D^0]/[D^+]$ is greater than 1 the very weak optical bias effect on the ESR measurements at room temperature reported in the literature[11] is accounted for. Thus, in the following, we consider the DB distribution of Fig. 1(b), and concentrate on the time variations of $\mu_n \tau_n$.

The results are shown in Fig. 2 for the two sets of electron capture cross sections already used in Table I. Figure 2(a) stands for $R = 5$, whereas Fig. 2(b) stands for $R = 100$. A first remark is that the results presented in Fig. 2 are in excellent agreement with the interpretation given by Antoniadis and Schiff on the electron-drift measurements.[13] The increase of $\mu_n \tau_n(t)$ at short times ($10^{-8} < t < 10^{-6}$ s) corresponds to the drift of electrons interacting with the conduction-band tail, the following ''plateau'' ($10^{-6} < t < 10^{-2}$ s) being due to deep trapping. Then the release of electrons from deep traps leads to a further increase of $\mu_n \tau_n(t)$ ($t > 10^{-2}$ s) followed by a plateau when the extra electrons have been recombined (the final value of $\mu_n \tau_n$ being lowered by the increase of F_{dc}, as expected). It is to be emphasized that, on one hand, the deep trapping is unchanged by the optical bias in Fig. 2(a), whereas, on the other hand, it is strongly decreased by increasing the optical bias in Fig. 2(b), resulting in a higher value of $\mu_n \tau_n$ or even in a suppression of the ''plateau'' for $10^{-6} < t < 10^{-2}$ s. Obviously, our calculated time dependence of $\mu_n \tau_n$ in Fig. 2(b) fairly agrees with all experimental trends reported in the literature.[9,10]

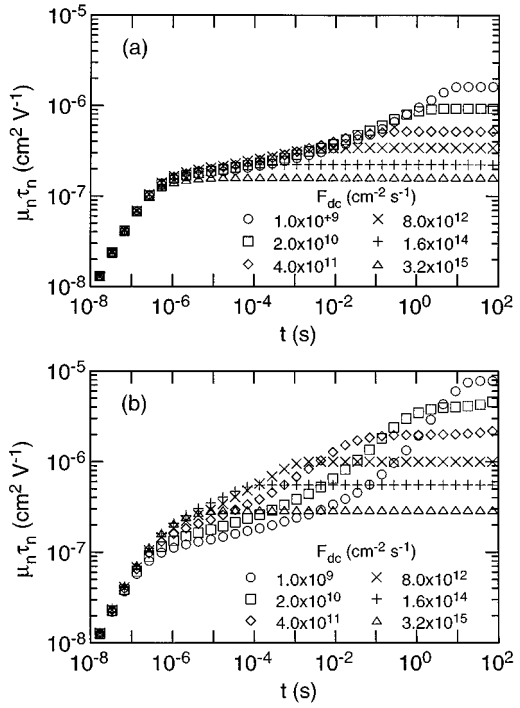

FIG. 2. Variations of $\mu_n\tau_n(t)$ calculated from the simulation of the transient electron-drift experiment with the DB distribution of Fig. 1(b). The results are shown for six values of the optical-bias photon flux F_{dc} (cm^{-2} s^{-1}): (○) 1.0×10^{9}, (□) 2.0×10^{10}, (◇) 4.0×10^{11}, (×) 8.0×10^{12}, (+) 1.6×10^{14}, (Δ) 3.2×10^{15}. In (a), the electron capture cross sections of charged and neutral dangling bonds are $\sigma_n^+=4\times10^{15}$ cm^2 and $\sigma_n^0=8\times10^{16}$ cm^2, so that the ratio $R=\sigma_n^+/\sigma_n^0=5$. The deep trapping is practically unaffected by the variations of F_{dc}. In (b), $\sigma_n^+=1\times10^{14}$ cm^2 and $\sigma_n^0=1\times10^{16}$ cm^2, so that $R=100$. The deep trapping is lowered by the variations of F_{dc} resulting in the suppression of the ''plateau'' observed for $10^{-6}<t<10^{-2}$ s.

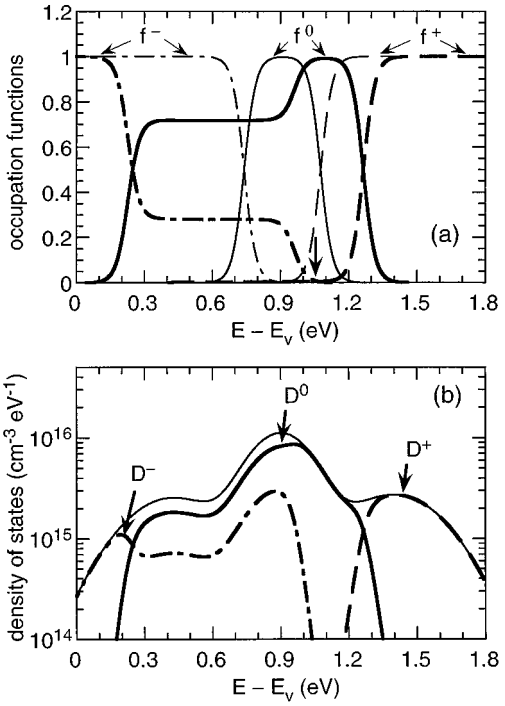

FIG. 3. (a) Comparison of the occupation functions f^+, f^0, and f^- for positively charged, neutral, and negatively charged dangling bonds (dashed, solid, and dash-dotted lines, respectively) in the dark (thin lines) and under an optical bias $F_{dc}=8\times10^{12}$ cm^{-2} s^{-1} (bold lines). The arrow indicates the position of the dark Fermi level. (b) Occupation of the dangling-bond distribution according to these occupation functions. The bold dashed, solid, and dash-dotted lines correspond to the positively charged, neutral, and negatively charged states, respectively. The thin solid line represents the whole DB density of states.

The evolution with the optical bias is due, first, to the fact that both D^0 and D^+ states play the role of deep electron traps, and, second, to the peculiar way the deep states are filled under optical bias, which is not as simple as a full conversion of D^0 into D^- or D^+ into D^0. In Fig. 3(a) we show the occupation functions calculated at $F_{dc}=8\times10^{12}$ cm^{-2} s^{-1} for the DB distribution of Fig. 1(b), with the second set of capture cross sections ($R=100$). In Fig. 3(b) the resulting occupation of the deep states is shown. From this figure three major points can be underlined:

(i) The energy range wherein neutral DB states can be found widens under the optical bias [see Fig. 1(b) for the comparison with the dark equilibrium state]. However, $[D^0]$ can remain practically the same as in equilibrium because the degree of neutral occupancy is lower than 1 in most of this energy range.

(ii) Due to this widening, some D^+ states are transformed into D^0 states. Since the capture cross section of neutral states is lower than that of charged ones, this results in a decrease of capture efficiency. This provides the explanation for the observed decrease in deep trapping leading to an enhanced electron-drift signal. This also explains why the effect is much more pronounced if the ratio R is increased.

(iii) Since $[D^0]$ remains practically constant under optical bias, the decrease of the final value of $\mu_n\tau_n$, reflecting an increase of recombination centers under increasing optical bias, indicates that the neutral dangling bonds do not necessarily provide the main contribution to the recombination. The different recombination paths associated with DB centers were analyzed in a previous paper,[12] where we showed that recombination also depends on the deepest D^+ states (see Fig. 6 of Ref. 12). Moreover, a significant contribution can also arise from the monovalent valence-band tail states, for they are partially emptied under high optical bias and therefore participate in the whole recombination process.[14]

In summary, the influence of the optical bias on the transient electron-drift measurements in a-Si:H along with the paradox raised by Han *et al.* (decrease of trapping efficiency though $[D^0]$ remains constant under optical bias) can be convincingly explained by a broad distribution of dangling bonds with more neutral than charged states, and a high ratio of the electron capture cross sections of positively charged and neutral defects. Thus, these optical-bias effects do not provide strong support for the slow relaxation theory in a-Si:H. We hope that our results will promote both electron-drift (or other conductivitylike) measurements and ESR measurements under optical bias (in particular, there is a lack of temperature-dependent ESR data under optical bias in the

literature). These kinds of experiments, if properly analyzed, appear very promising to get a more precise knowledge of the distribution of defects and their capture cross sections in *a*-Si:H.

We thank E. A. Schiff for stimulating discussions and G. Fournet for his careful reading of the manuscript. Laboratoire de Génie Electrique de Paris is ''Unité associée au Centre National de la Recherche Scientifique No. D0127.''

[1] M. J. Powell and S. C. Deane, Phys. Rev. B **48**, 10 815 (1993).
[2] G. Schumm, Phys. Rev. B **49**, 2427 (1994).
[3] K. Hattori, M. Anzaï, H. Okamoto, and Y. Hamakawa, J. Appl. Phys. **77**, 2989 (1995).
[4] N. Wyrsch and A. Shah, J. Non-Cryst. Solids **137&138**, 431 (1991).
[5] A. Mittiga, P. Fiorini, L. Fornarini, M. Petracca, and G. Grillo, Philos. Mag. B **70**, 277 (1994).
[6] R. H. Bube, L. E. Benatar, M. N. Grimbergen, and D. Redfield, J. Appl. Phys. **72**, 5766 (1992).
[7] F. Zhong and J. D. Cohen, Phys. Rev. Lett. **71**, 597 (1993).
[8] R. Pandya and E. A. Schiff, J. Non-Cryst. Solids **59&60**, 297 (1983).
[9] X. Chen and C.-Y. Tai, Phys. Rev. B **40**, 9652 (1983).
[10] D. Han, D. C. Melcher, E. A. Schiff, and M. Silver, Phys. Rev. B **48**, 8658 (1993).
[11] S. Zafar and E. A. Schiff, Thin Solid Films **164**, 239 (1988); see also Z. M. Saleh, H. Tarui, N. Nakamura, M. Nishikuni, S. Tsuda, S. Nakano, and Y. Kuwano, Jpn. J. Appl. Phys. **31**, 3801 (1992).
[12] C. Longeaud and J. P. Kleider, Phys. Rev. B **48**, 8715 (1993).
[13] H. Antoniadis and E. A. Schiff, Phys. Rev. B **46**, 9482 (1992).
[14] G. W. Taylor and J. G. Simmons, J. Non-Cryst. Solids **8-10**, 940 (1972).